

Deformation of a foreland carbonate thrust system, Sawtooth Range, Montana

JAMES E. HOLL
DAVID J. ANASTASIO } *Department of Earth and Environmental Sciences, Lehigh University, Bethlehem, Pennsylvania 18015-3188*

ABSTRACT

An analysis of mesoscale faulting associated with thrust-belt development was completed along a transect crossing several foreland thrust sheets of the central Sawtooth Range, Montana. At a regional scale, a balanced cross section of the central Sawtooth Range, constrained by well, seismic, and surface data, indicates a minimum of 60% horizontal shortening of the upper Paleozoic carbonate bank sequence, accommodated by a forward-developing thrust system. Subsurface data delineates a 4° westward-dipping Precambrian basement and westward thickening of the Precambrian Belt Supergroup. Major décollements within the central Sawtooth Range are present at the base of the Devonian Jefferson Formation, in the lower Mississippian Allan Mountain Limestone, and in the Cretaceous Colorado Group.

Within the Diversion, French, Norwegian, and Beaver thrust sheets of the central Sawtooth Range, deformation has been partitioned into arrays of meter- to decimeter-sized faults that constitute brittle deformation zones (BDZs). BDZ thickness is directly related to fault displacement but is not related to fault trajectories or subsequent foreland imbrication. The ratio of BDZ thickness to displacement is nearly constant, with BDZ thicknesses ranging from 65 m to 200 m for faults whose displacements range from 2 km to 5 km. The BDZs of each thrust sheet can be separated into three regions defined by differences in fault diversity, fault intensity, and fault kinematics. Proportionally, the locations of boundaries between regions within the BDZs are remarkably constant for each of the four thrust sheets studied, indicating that the BDZs widen uniformly during thrust sheet emplacement. BDZ bases are characterized by an interlocking network of faults that exhibit great diversity and accommodate mesoscale cataclastic flow. BDZ bases are domi-

nated by oblique-slip faults, whereas the middle and upper regions of BDZs are dominantly dip- or strike-slip faults. In all regions of a BDZ, localized zones of contractional, extensional, or more commonly, transport-parallel strike-slip faults bounded by bedding-plane detachments are present. Fault length/m² of outcrop decreases logarithmically to zero from a maximum of 4 m/m² across the French and Norwegian BDZs. Zones of intense faulting alter this general pattern of decreasing fault intensity in the Diversion and Beaver thrust sheets.

INTRODUCTION

The Sawtooth Range in Montana exemplifies an imbricate thrust geometry common to external portions of mountain belts (Mudge, 1972; Lageson, 1987; Fig. 1). In such foreland regions of mountain belts, deformation typically occurs at sub-greenschist grade conditions, and thrust faults and fault-related folds dominate regional structures. On a mesoscopic scale, rocks within foreland areas of mountain belts typically deform by discontinuous mechanisms such as fracturing and faulting (Wojtal, 1986).

A balanced cross section (Elliott, 1983) across the central Sawtooth Range was constructed using surface data and available well and seismic data. The cross section constrains fault shapes, the amount of individual fault displacement, and the amount of stratigraphic thickening and horizontal shortening. The geometry provided by the deformed and restored cross sections also provides a framework for consideration of mesoscale deformation within the range.

Deformation features within the frontal thrust sheets of the central Sawtooth Range are dominated by mesoscale fault arrays that define brittle deformation zones (BDZs) associated with each regional thrust sheet. Previous work has established that minor fault fabrics indicate the kinematic history of thrust-sheet emplacement

and has resulted in some progress toward understanding the manner in which discontinuous deformation is partitioned within foreland thrust sheets. Price (1967) determined the relative movement directions within two converging structural salients and characterized a transverse fault using minor fault arrays within Front Range thrust sheets of the Southern Canadian Rocky Mountains. Farther north in the Front Ranges, Bielenstein (1969) used plan view variations in minor faults to document strike-parallel extensional strains during thrust-sheet emplacement. Wojtal (1986) analyzed the minor fault populations within three Appalachian thrust sheets and found that mesoscale deformation occurred in two components. First, the rock was shortened subparallel to the transport direction and thickened by low-angle, synthetic reverse faults. Second, the sheet was extended both subparallel and normal to transport and thinned by high-angle, foreland-dipping normal faults.

In addition to use in kinematic studies, minor fault arrays can be used to determine the orientation and magnitude of the pervasive mesoscale strain if fault displacements and attitudes are known (Wojtal, 1986, 1989). If only the fault orientation, sense, and direction of slip are known, and if assumptions are correct about the relationship between stress directions and fault orientation (Anderson, 1951; Reches, 1978), then it is possible to estimate the orientation of principal-stress axes (Wallace, 1951; Arthaud, 1969; Angelier, 1979; Etchcopar and others, 1981; Aleksandrowski, 1985; Reches, 1987; Wojtal and Pershing, 1991), and it may be possible to determine their relative magnitudes (Angelier, 1984, 1989; Wojtal and Pershing, 1991).

In order to better understand BDZ development within foreland thrust sheets, four well-exposed thrust sheets of varying structural position and displacements within the frontal region of the central Sawtooth Range, Montana (Fig. 1), were studied. The Diversion, French, Norwegian, and Beaver thrust sheets were se-

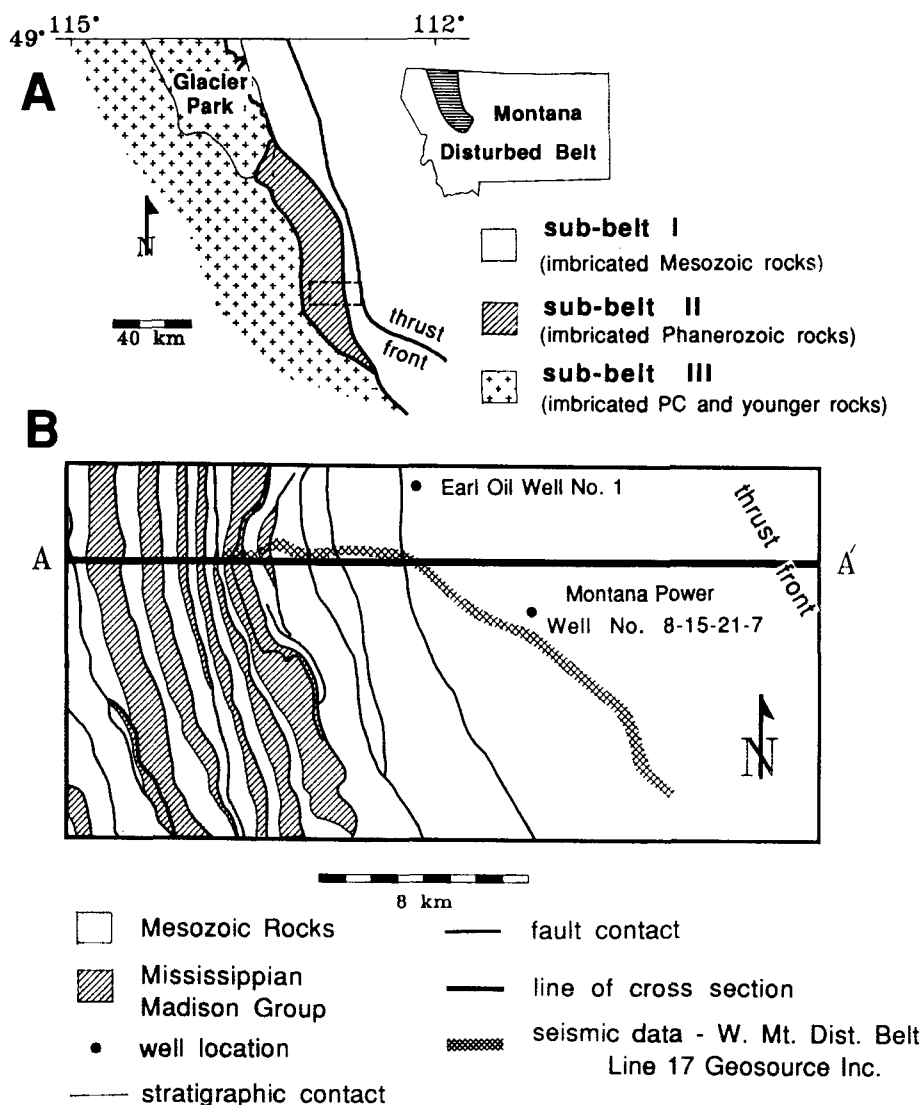


Figure 1. (A) Generalized geologic map of the Montana Disturbed Belt. (B) Geologic map of the central Sawtooth Range (after Mudge, 1965, 1966, 1982, 1983; cross section A-A' shown in Fig. 5).

lected because of the variety of exposure orientations produced along roadcuts and the Sun River (Fig. 2) and the irregular, continuous nature of the outcrops. The nature of the exposures allowed sampling of the minor fault populations in three dimensions, thus maximizing data available to investigate fault-zone processes.

Potential variables controlling the internal deformation of a thrust sheet are hanging-wall and footwall rock types, fault displacement, and distance from the fault's lateral terminations. In the central Sawtooth Range, by selecting thrust sheets that had similar hanging-wall and footwall rock types, it was possible to isolate displacement and distance from the lateral termina-

tions of faults in an analysis of fault-zone processes. In the hanging walls of each thrust sheet, mesoscale structural data were collected throughout the continuously exposed Mississippian sections.

Faults within the frontal thrust sheets of the central Sawtooth Range are generally coated with shear fibers, indicating pressure solution slip (Elliott, 1976). Shear fibers were interpreted to determine the direction and sense of slip for each fault surface. After Norris (1958), contraction faults are defined as those that shorten bedding, and extension faults are those that extend bedding. For this study, faults with movement direction within 30° of the minor faults' intersec-

tion with bedding were considered strike-slip faults. Using these criteria, eight classes of faults are possible (Fig. 3); these faults result in range-parallel or range-perpendicular contraction, extension, or strike-slip. Each of these fault types developed during the emplacement of the thrust sheets of the central Sawtooth Range.

The results of the mesoscale analyses were compared with fault shapes, fault displacements, and position within the thrust belt to establish controls on thrust-sheet deformation. These analyses provide insight into fault-zone evolution and the kinematics of thrust-sheet emplacement.

GEOLOGIC SETTING

Structural Setting

The Montana Disturbed Belt (Fig. 1) is a segment of the U.S. Rocky Mountains. The Rocky Mountains in west-central Montana are characterized by three subbelts. From west to east these include Subbelt I, containing imbricated Precambrian and younger rocks; Subbelt II, which is comprised of Paleozoic and younger imbricates; and Subbelt III, which contains imbricated synorogenic Mesozoic rocks (Mudge, 1982). The central Sawtooth Range is an arcuate zone of north-trending, closely spaced, westerly dipping, imbricate thrust sheets and associated folds which compose Subbelt II in the vicinity of the Sun River. The central Sawtooth Range formed in the Late Cretaceous to early Paleocene during the Sevier orogeny (Mudge, 1970).

Stratigraphy

The Sawtooth Range exposes Paleozoic and Mesozoic sedimentary rocks (Fig. 4). Underlying the Sawtooth Range, the Precambrian Belt Supergroup consists of marine siliciclastic rocks with subordinate carbonate units. The Cambrian and Devonian stratigraphic sequence consists predominantly of carbonate rocks, with relatively few thin siliciclastic units. The Devonian strata also contain evaporite-solution breccias. Overlying the Devonian units are Mississippian carbonate rocks of the Allan Mountain Limestone and Castle Reef Dolomite. These units are interbedded marine limestone and dolomite, with the percentage of dolomite increasing up section. Jurassic and Cretaceous marine and non-marine, foreland-basin, siliciclastic strata that are partly synorogenic unconformably overlie the Mississippian carbonate rocks (Mudge, 1982). The focus of this study is mesoscale faulting within the Allan Mountain Limestone and Castle Reef Dolomite exposed within the hanging walls of the Sawtooth thrust sheets.

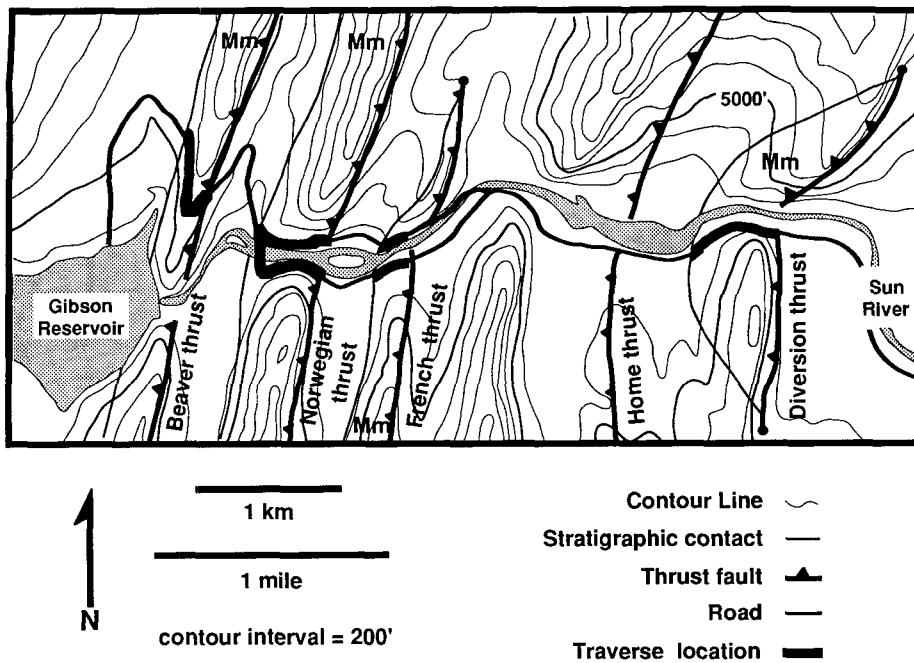


Figure 2. Topographic map of the Sun River Canyon area showing regional thrust faults and the locations of the traverses through the thrust sheets.

REGIONAL SCALE DEFORMATION

A balanced cross section was constructed through Subbelts I and II of the Montana Disturbed Belt. The balanced cross section defines the geometry of the Sawtooths, the amount of regional scale shortening, and individual thrust-sheet displacement (Fig. 5). The eastern edge of this cross section was pinned in undeformed rocks of the foreland.

Regional deformation within the Devonian and Mississippian units of Subbelt II is characterized by imbricate thrust faults and concomitant folding (Fig. 5). Major décollement surfaces are at the base of the Devonian Jefferson Formation and at the top of the lower member of the Mississippian Allan Mountain Limestone (Fig. 4). The style of deformation within the Jurassic and Cretaceous rocks of Subbelts I and II is characterized by abundant imbricate thrust faults with relatively small offsets (Mudge, 1982; Johnson, 1988) and tight asymmetric folds, with major décollement surfaces in the Cretaceous Colorado Group. Deformation within Subbelt I has been described by Mudge (1972) and Johnson (1988).

Underlying the allochthonous rocks, the Belt Supergroup ranges in thickness from ~400 m at the thrust front to >600 m at the western edge of Subbelt II. The thickness estimate was determined by correlating a regional seismic reflection line to an exploration well log that

penetrated the top of the Cambrian Devils Glen Dolomite. Time-to-depth conversions were based on reported migration velocities. Published estimates of the thickness of Cambrian rocks (Mudge, 1982) were used to locate the top of the Precambrian Belt Supergroup. The thickness of the belt was taken as the difference between the top of the Belt Supergroup and a seismic interpretation of the basement cover sequence interface. Our thickness estimates closely agree with the 500 m shown on Mitra's (1986)

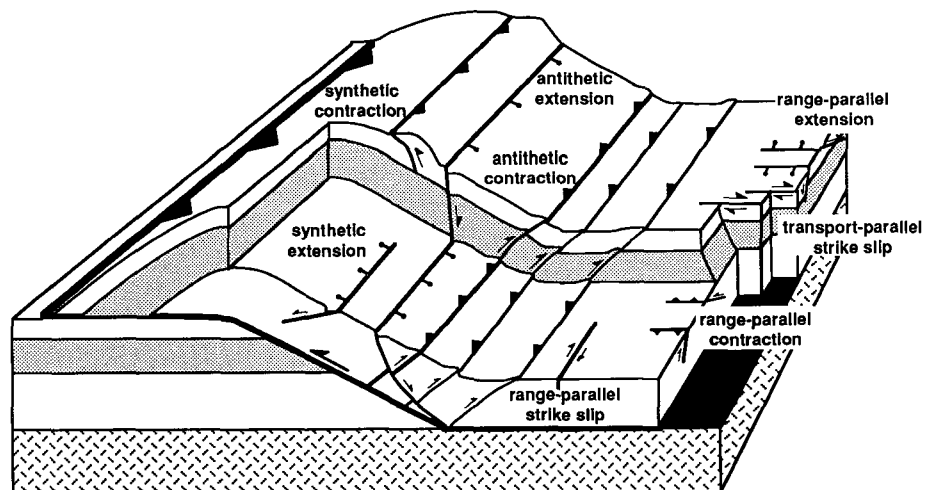


Figure 3. Schematic thrust sheet defining mesoscale fault types.

cross section through the Sawtooth Range but are substantially less than the 2,000 m reported by Mudge and others (1982). A dip of 4° west for the underlying Precambrian crystalline basement was determined from several variously oriented, regional seismic profiles. This estimate of basement dip is comparable to the 3° – 4° reported by Bally and others (1966) for the Canadian Rockies. The calculated dip, however, is more than the 2° – 3° determined from regional structure contour maps of the top of Precambrian crystalline rocks constructed by projecting the depth to basement from well logs that penetrate only into the Paleozoic section (Mudge, 1982).

Continuous structural profiles were conducted through the Diversion, Norwegian, French, and Beaver thrust sheets. The traverses along the Sun River allowed an assessment of along-strike variation in fault-zone development (Fig. 6). The thrust sheets of the central Sawtooth Range have simple fault trajectories (Fig. 5). Field and map observations indicate that the thrust faults and bedding within the overlying Mississippian Allan Mountain Limestone are parallel within the Diversion, Norwegian, and Beaver thrust sheets for many kilometers along the strike of the fault. From field and map evidence (Mudge, 1965, 1966; Mudge and others, 1982; Mudge and Earhart, 1983; this study) we infer that the primary detachments for the Diversion, French, Norwegian, and Beaver thrust sheets along the Sun River transect lie in the Mississippian Allan Mountain Limestone and in the Cretaceous Colorado Group, with a major 20° frontal ramp connecting the two flats.

The minimum slip required to restore the paleozoic section back to regional position was chosen and ranged from ~2–5 km for the four

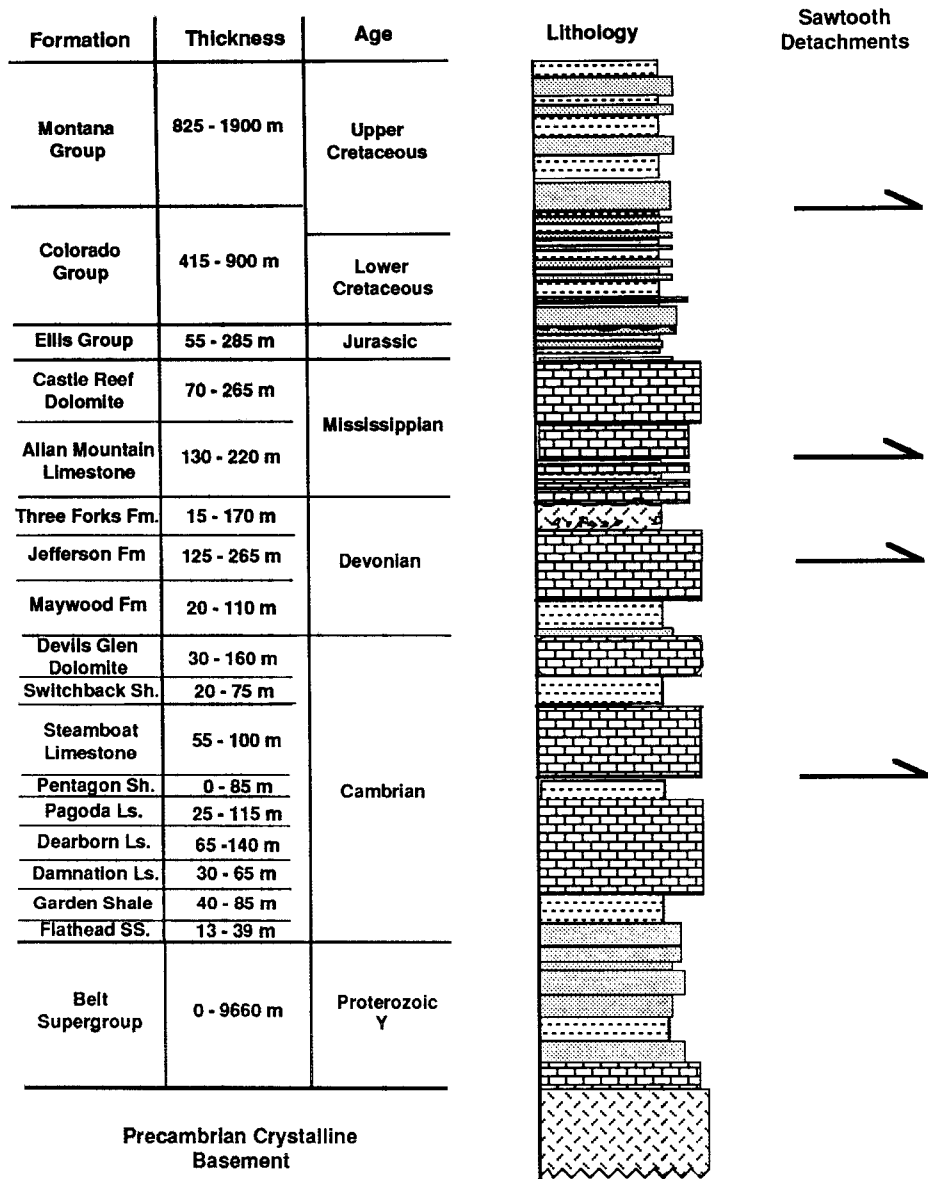


Figure 4. Stratigraphic column for western Montana (after Mudge, 1982). The primary horizons of Sawtooth detachments are indicated.

thrust sheets (Fig. 5). Errors in the estimates of fault displacement were determined on the basis of the variance of calculated displacements on several admissible (Elliott, 1983) versions of the cross section. The minimum horizontal shortening of the Paleozoic carbonates from the thrust front to the trailing branch line of the Beaver thrust fault is ~60% (15 km).

MESOSCALE DEFORMATION

Deformation at the base of each thrust sheet of the central Sawtooth Range was partitioned into arrays of mesoscopic faults that define BDZs. Individual minor faults found at any po-

sition within any of the thrust sheets are indistinguishable; however, fault spacing, attitude, and slip direction change systematically with distance above each regional thrust. At comparable positions within the Sawtooth BDZs, minor fault arrays record similar kinematic patterns, suggesting that arrays of minor faults and not individual faults are the primary components of mesoscale deformation. The kinematic patterns recorded by minor fault arrays provide insight into foreland fault-zone development.

The BDZs within each of the thrust sheets are defined as the region in each thrust sheet between the regional thrust surface and the last observed minor fault within the hanging wall.

BDZ thickness was measured normal to the regional thrust. The total thickness of each BDZ along the Sun River transect varies directly with thrust-sheet displacement (Fig. 7). As fault displacement increases from 2 km on the Diversion thrust to ~5 km on the more hindward Beaver thrust, BDZ thickness increases linearly from 65 m to 200 m. A line of best fit for the data was calculated, using linear regression, and indicates that the ratio of BDZ width to thrust sheet displacement was approximately 1:22 for all four thrust sheets (Fig. 7). The thickness of the BDZ does not correlate with differences in fault shape (ramp/flat ratio) or the number of foreland imbricates that carried more hinterland sheets piggyback. Although displacement is the dominant factor controlling BDZ development, position above the regional thrust and relative distance from the faults' lateral terminations control the kinematic patterns observed.

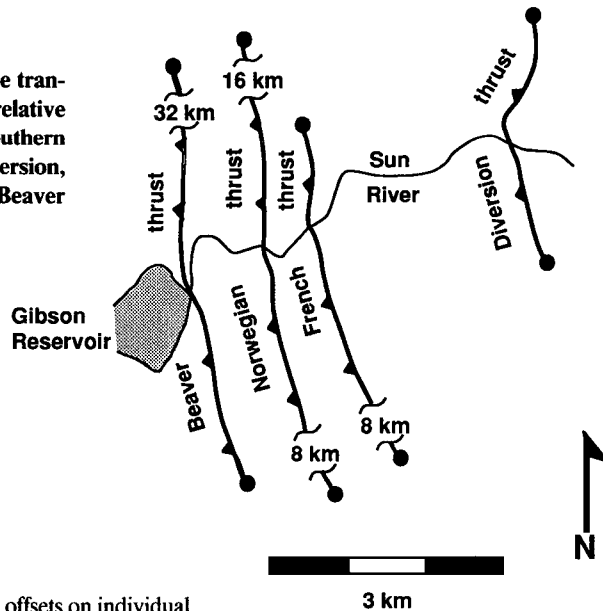
Because of the massive character of the Paleozoic section, it was not possible to measure fault displacement on more than 10% of the faults observed. Using faults where displacement was apparent, we investigated the relationship between fault length and displacement. Although there is a general logarithmic increase in offset with increasing fault length, the relationship is not useful for calibrating fault displacements due to large variance in the data (Fig. 8). Our inability to define an empirical relationship between displacement and fault length made it impossible to precisely determine the amount of penetrative strain partitioned into mesoscale faulting. In order to quantify the relative intensity of mesoscale deformation, the total fault length/m² of profile was determined across each thrust sheet (Fig. 9). Fault length/m² was calculated every 25 m by direct measurement of the total fault length exposed within a 10 m² area of outcrop. From these data it is apparent that fault intensity is always higher at the base of a BDZ than at the top. The decrease in fault intensity is sometimes irregular. In the French and Norwegian thrust sheets the intensity of mesoscale deformation decreases logarithmically from 4 m/m² to 0 m/m² away from the thrust surface. In the Diversion and the Beaver thrust sheets the pattern is more complicated. Zones of more intense faulting within the BDZ occur, producing peaks in the overall pattern (Fig. 9).

In order to characterize the kinematic patterns within the BDZs, slip linear plots were used (Fig. 10; Hoepfener, 1953; Anastasio, 1987; Twiss and Geffell, 1991). Slip linears preserve fault attitude, slip direction, and sense of movement by stereographically plotting a segment of the great circle (M-plane) that contains the fault pole and the slip direction, and an arrowhead that records the relative direction of fault slip.

Systematic changes in fault intensity and kinematics allow us to partition each BDZ into three regions. Within each BDZ, we recognized distinct groups of minor faults having similar orientations and slip directions. Collections of minor fault groups define the kinematics of the meso-scale deformation within each region of a BDZ.

Using the Bingham axial distribution technique, we determined an average slip linear for groups of minor faults having similar attitudes and movement directions at different levels within each BDZ. M-planes and the fault planes were averaged in order to construct an average slip linear plot. Averages were considered valid if eigenvalues for both averages exceeded 0.80 when accounting for >80% of the faults in an analysis. An example data reduction from the middle part of the Diversion BDZ is shown in Figure 11, with the accompanying statistical parameters describing the data clustering presented in Table 1. Summary slip linear plots of meso-scale faults allow the clarification of the kinematics of deformation while quantifying the natural variation in the data. The results of the data reduction are displayed as block diagrams. The block diagrams provide the clearest visual display of fault spatial variations, fault orientations, sense of movement, and relative abundances within each BDZ.

Figure 6. Position of the transect along the Sun River relative to the northern and southern terminations of the Diversion, French, Norwegian, and Beaver thrust sheets.



It is possible that because offsets on individual minor faults are not known, kinematic analyses may be skewed towards numerically dominant fault types. This would occur when fault types with the highest density do not make the largest contribution to the total displacement field, which is possible when one or several of the numerically subordinate fault types are of large displacement. This does not appear to be the case within the central Sawtooth Range, how-

ever, because fault types that dominate numerically also contribute the largest fraction of total fault length within a given region of the BDZ.

Data recorded in continuous traverses across each BDZ fall into three regions defined by differences in fault type and intensity (Fig. 12). The boundaries between regions within the BDZ are gradational. For the four thrust sheets studied,

Figure 5. Restored and deformed balanced cross sections along A-A' through the central Sawtooth Range (see Fig. 1 for line of section). Deformation within the upper Cretaceous is depicted schematically.

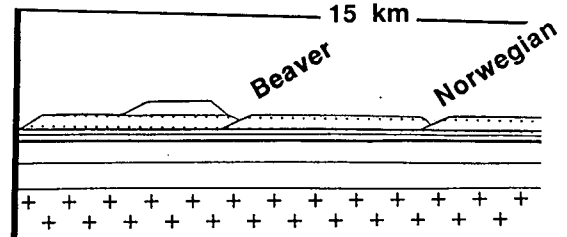


Figure 7. Graph of BDZ thickness and region boundaries versus regional thrust displacement.

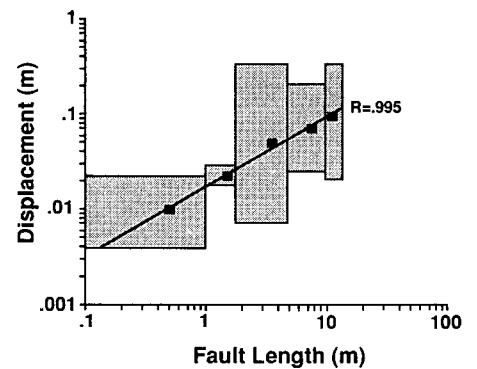
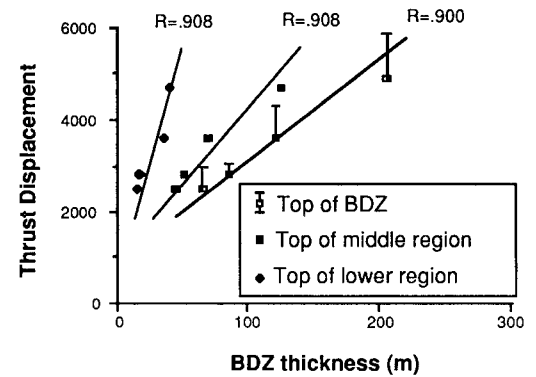


Figure 8. Graph of minor fault length versus displacement for the limited number of minor faults where it was possible to estimate offsets. Mean fault displacements for fault classes of .1–1 m, 1–2 m, 2–5 m, 5–10 m, and >10 m are indicated by a solid square. The horizontal side of each shaded box represents the range in fault length considered in each fault class, while the vertical side represents the range in measured displacements for each fault class.

the boundaries between the lower and the middle regions and the middle and upper regions range 18%–23% and 60%–70% of the total BDZ thickness, respectively (Fig. 12).

Although the pattern of mesoscale deformation in each thrust sheet varied, some generalizations concerning the kinematics of Sawtooth

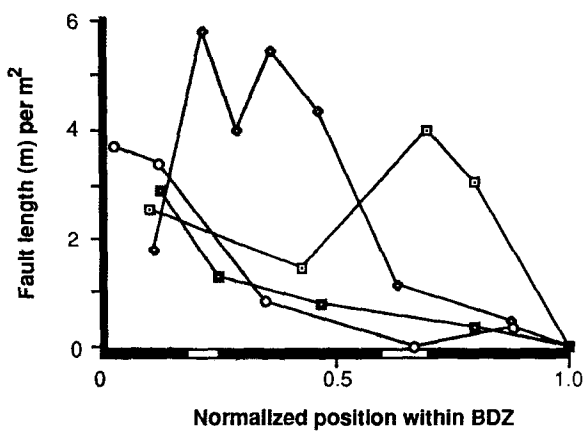
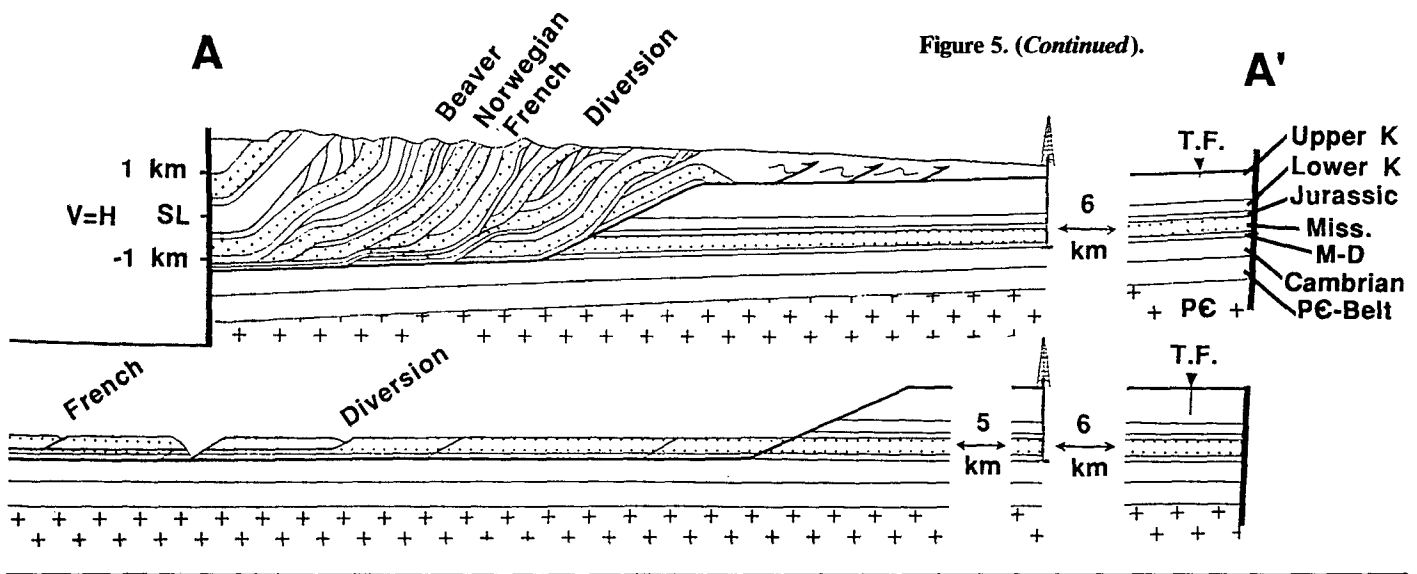


Figure 9. Plots of total fault length per meter squared as a function of distance from the base of the thrust sheet for the Diversion, French, Norwegian, and Beaver thrust sheets of the central Sawtooth Range.

TABLE 1. STATISTICAL DATA DESCRIBING THE CLUSTERING OF DATA POINTS FOR THE FAULT POPULATIONS SHOWN IN FIGURE 11

Population	N	% total	k faults	k M-planes
A	50	50%	.81	.82
B	22	22%	.85	.80
C	19	19%	.97q	.90
D	8	8%	.86	.82

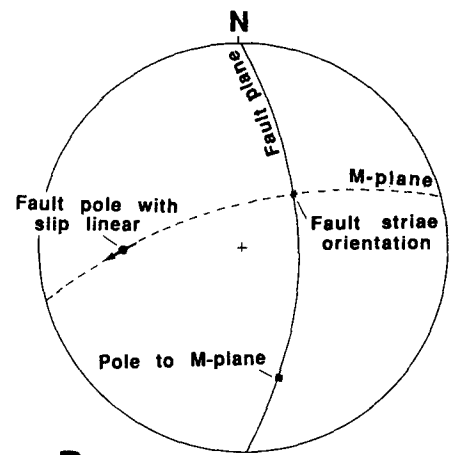
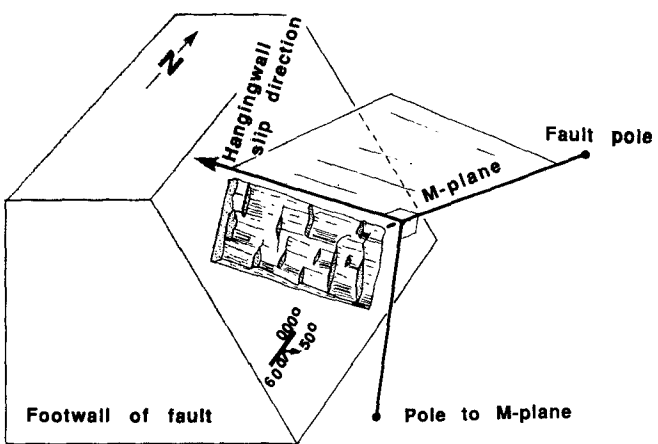


Figure 10. (A) Block diagram of the commonly analyzed kinematic features on a fault plane. (B) An equal area plot of the slip linear and the great circle traces of the fault plane and M-plane (from Anastasio, 1987).

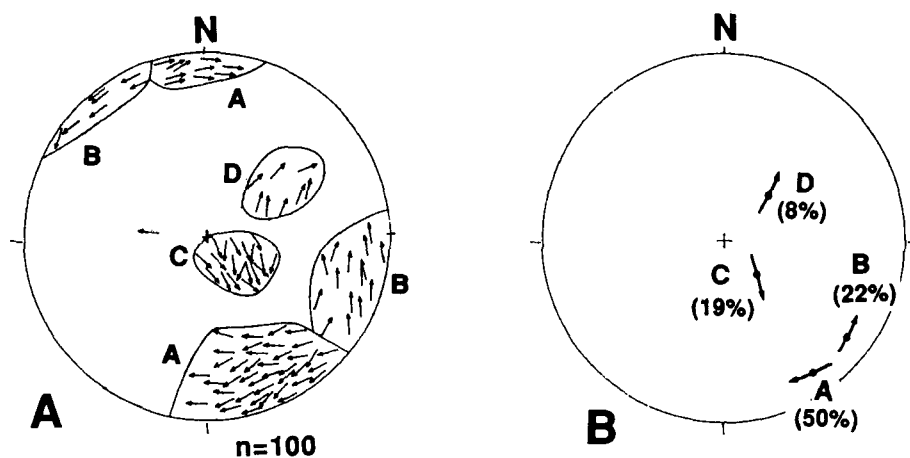


Figure 11. (A) A slip-linear plot of minor faults found within the middle region of the Diversion BDZ. (B) Reduced data with the percentage of data points projected into each slip linear indicated.

minor faults found at the base of the BDZs are range-parallel contraction faults with oblique slip; range-parallel, strike-slip faults; and transport-parallel, strike-slip faults (Fig. 14). Few faults at the base of any of the BDZs studied record dip-slip movement. While limited, cross-cutting relationships observed at the bases of all four thrust sheets suggest that all populations of minor faults were active contemporaneously.

In the middle region of each BDZ, there is an abrupt decrease in fault diversity manifested by a loss of minor faults with range-parallel motion. Transport-parallel strike-slip, contraction, and extension faults are most common in the middle region of a BDZ (Figs. 14 and 15) and may be localized into relatively thin zones of intense faulting. In the middle region of the Diversion and Beaver BDZs, the most prevalent type of minor faults are transport-parallel, strike-slip

faults (Fig. 15). The middle of the Norwegian and French BDZs contain a substantial percentage of transport-parallel contraction and extension faults, but transport-parallel, strike-slip faults are conspicuously absent.

The top of each BDZ is characterized by a low diversity of minor fault types and is dominantly dip- or strike-slip, including transport-parallel contraction and extension faults (Figs. 14 and 15). As in the middle region of the BDZs, transport-parallel, strike-slip faults are common in the Diversion and Beaver BDZs.

Transport-parallel, strike-slip faults are the most penetrative class of minor faults observed within the BDZs (Figs. 14 and 15). Both right- and left-lateral faults are common in the same fault arrays; however, one movement sense dominates depending on the lateral position within the thrust sheet. In locations north of the

middle of a thrust sheet, left-lateral faults dominate, whereas in locations toward the southern tip, right-lateral faults dominate.

DISCUSSION

Mesoscale Deformation

Deformation of four of the frontal imbricates of the Sawtooth Range was strongly partitioned into mesoscale fault arrays that define BDZs along each regional thrust fault. Penetrative grain-scale strain was uniformly low across each thrust sheet studied (Holl, 1991). The ratio of BDZ width to displacement is relatively constant for all four thrust sheets studied. Linear relationships between fault-zone thickness and fault displacement have also been reported by Robertson (1983) and Otsuki (1978). Hull (1988) resolved a general relationship between thickness and displacement for deformation zones that varied in size by over seven orders of magnitude. The ratio of fault zone thickness to displacement for these deformation zones varied between 10 and 1,000 and averaged 1:63 (Hull, 1988; Evans, 1990). These studies included data from a wide range of rock types and structural conditions, which may explain the wide variance in the ratios of fault-zone thickness to displacement observed (Evans, 1990). Within the central Sawtooth Range, we define a correlation between BDZ thickness and displacement for thrust sheets that contain the same hanging-wall carbonate rocks and footwall sandstone and shale and have deformed under foreland conditions. This relationship indicates a temporal and genetic link between displacement and BDZ development.

Wojtal (1986) and Wojtal and Mitra (1986) suggested that BDZs develop progressively. As thrust faults develop, an interlocking network of mesoscale faults form which divide the base of the sheet into meter- or decimeter-size blocks (Stearns, 1969). During continued displacement, deformation is accommodated by additional mesoscale faults and intrablock accommodation features, such as fractures and veins. These intrablock deformation features may, with continuing thrust-sheet displacement, develop into mesoscale faults. The density of minor faults near a fault will eventually reach a limiting value. Further deformation would be accommodated by increased displacement on existing minor faults or by thickening of the BDZ (Wojtal and Mitra, 1986).

The uniformity in relative thicknesses for lower, middle, and upper regions of the BDZs in the Sawtooth thrust sheets suggests that the BDZs widen uniformly with increased displacement. Areas once near the top of a BDZ,

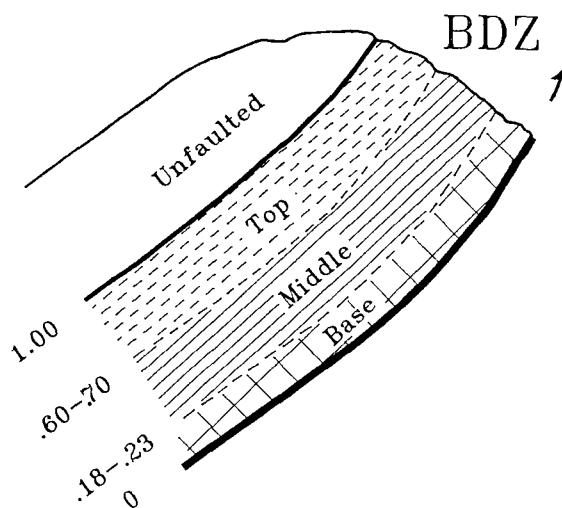


Figure 12. Schematic BDZ showing subdivision boundaries. Percentages represent the range in position of subdivision boundaries as a function of total BDZ thickness for studied Sawtooth Range thrust sheets. Similar hatching patterns are used in subsequent figures to denote position within the BDZ.

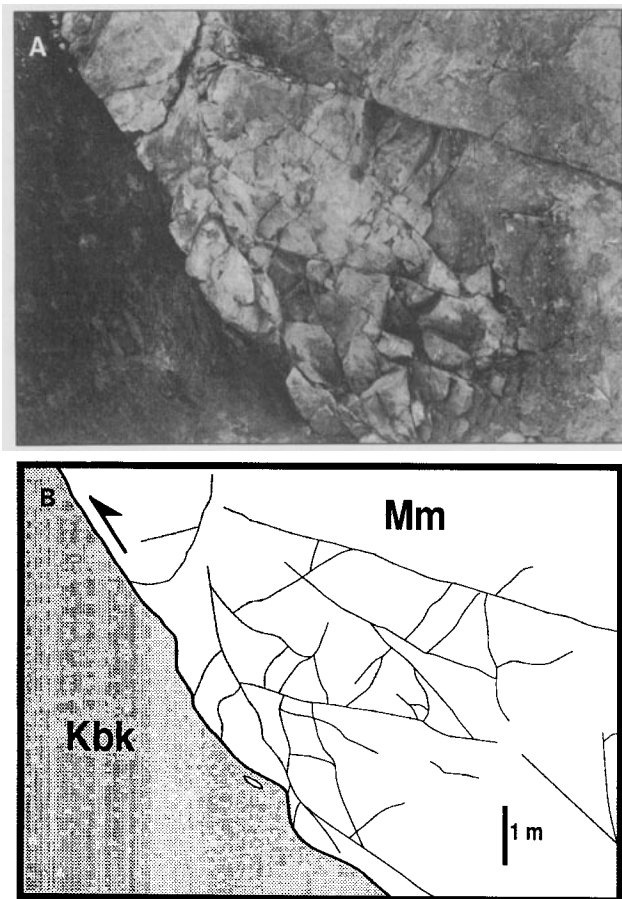


Figure 13. View south of the French thrust. The figure shows the high quality of exposures available within the Sun River Canyon and the diversity, intensity, and connectivity of the minor faults within the base of the hanging-wall BDZ. The minor fault network allows the base of the thrust sheet to deform by meso-scale cataclastic flow. (Mm, Mississippian Madison Group, Kbk, Cretaceous Blackleaf Fm.)

become incorporated into lower regions as the BDZ widens, overprinting previously developed faults. This is in contrast to Wojtal and Mitra's (1986) model of progressive thrust-sheet deformation. Within the upper and middle zones of the BDZs, minor faults are more diffuse than at the base and do not appear to be strain hardening the BDZ through interference with each other. Our observations suggest that fault zones widen before the existing BDZ is saturated with minor faults.

In thrust sheets of the southern Appalachians, 15–20 km of displacement resulted in the development of fine-grained, foliated cataclasite in the blocks within 10 m of a regional thrust fault (Wojtal, 1986; Wojtal and Mitra, 1986). The reduction in grain size promoted other grain-size-sensitive deformation mechanisms, such as pressure solution. This resulted in strain softening at the base of the thrust sheet, allowing further displacement to be accommodated along the regional detachment without proportional increases in the thickness of the developing fault zone. This strain-softening process is apparent when comparing the size of brittle deformation zones versus displacement for thrust sheets studied by Wojtal (1986) to the thrust sheets of the central Sawtooth Range. For a thrust sheet having a displacement of 1–2 km, Wojtal measured a BDZ thickness of 90 m, which matches well with correlations for the central Sawtooth Range (Fig. 7). For a thrust sheet with an estimated displacement of 15–20 km, however, the measured BDZ thickness of 350 m is significantly lower than what would be predicted by our empirically derived relationship (Fig. 7). In the Sawtooths, the linear relationship between BDZ thickness and thrust displacement suggests that these BDZs were rheologically constant and did not develop strain-softening behavior.

The kinematics of minor faulting within the central Sawtooth Range delineates three types of mesoscale strain. Transport-parallel bulk shear is accommodated by transport-parallel, strike-slip faults. These faults likely result from lateral variations in thrust-sheet displacement. The sense of a transport-parallel, strike-slip fault that dominates a fault array depends on lateral position within the thrust sheet. This observation is compatible with Elliott's (1976) bow and arrow model of thrust-sheet displacement, which suggests that the middle parts of a thrust sheet are active longest and are displaced the farthest (Fig. 16). In order to accommodate this differential movement within the Sawtooth Range, zones of mesoscale, transport-parallel, strike-slip faults may have developed with left-lateral faults dominating in the northern parts of a thrust sheet and right-lateral, transport-parallel strike slip dominating in the south. Alternatively, the develop-

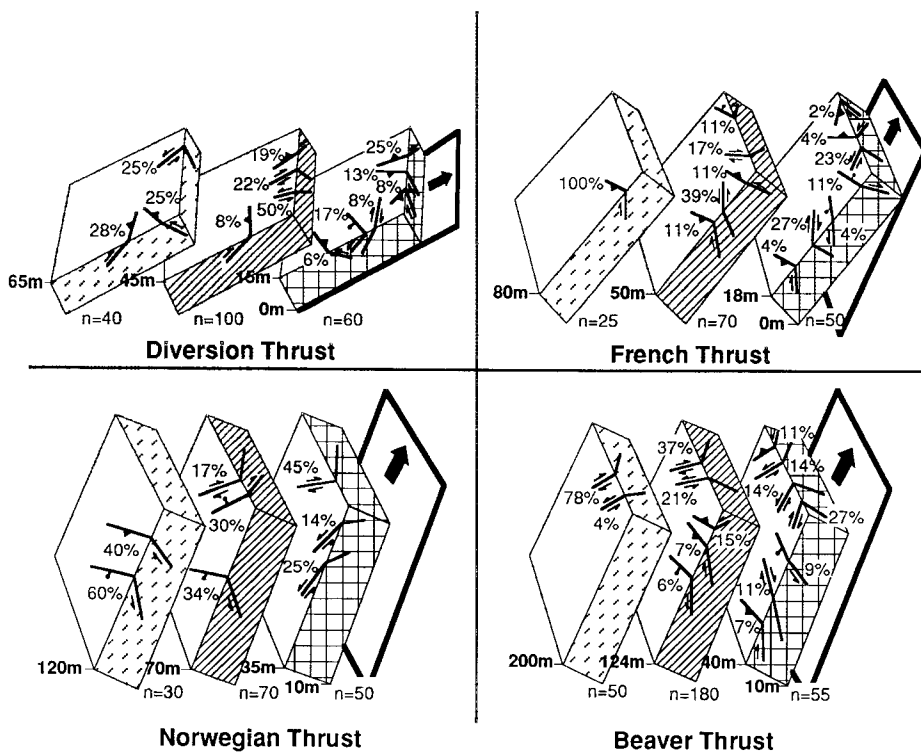


Figure 14. Block diagrams summarizing the distribution of minor faults across each BDZ.

ment of localized zones of transport-parallel, strike-slip faulting may be related to local heterogeneities within the thrust sheet or variable tractions along the base of the thrust sheet.

Transport-parallel, strike-slip faults are present throughout each BDZ and generally contribute the most fault length to the total fault intensity, particularly within the middle and upper parts of the BDZs. These observations suggest that lateral variations in fault displacement or localized heterogeneities within the thrust sheet may be the most significant strain being partitioned into minor faults. In the Diversion and Beaver thrust sheets, large peaks in total fault intensity are associated with large increases in transport-parallel, strike-slip faults, suggesting that our transect across the Sawtooths included local zones of concentrated transport-parallel, strike-slip faulting.

A second type of meso-scale strain accommodated within these BDZs is range-parallel contraction and extension. Range-parallel extension is generally accommodated within the lowest region of a BDZ and, where exposed, is separated from the remainder of the BDZ by a zone of strike-parallel extension. These zones of strike-parallel displacement may be the result of movement of the hanging wall over asperities in the footwall (Fig. 16). The decrease in the overall diversity of minor fault populations across a BDZ is the result of the localization of strike-parallel motion near the base of the BDZ. This localization of range-parallel extension suggests that the thrust sheet may accommodate asperities relatively near its base.

Shortening and thickening of the thrust sheets of the central Sawtooth Range are manifested by the presence of synthetic and antithetic contrac-

tion and extension faults in the BDZs. These fault types may be attributed to heterogeneous simple shear within the thrust sheet (Serra, 1977; Wojtal, 1986; Woodward and others, 1988). Zones of contraction and extension within the Sawtooth thrust sheets allow parts of the thrust sheet to be thickened or thinned and may be related to variable tractions along the thrust-fault surface during slip (Platt and Leggett, 1986) or along bedding-plane detachments within the thrust sheet.

The character of the minor fault arrays in the Norwegian thrust sheet differs from the other Sawtooth thrusts. The lack of faults that accommodate range-parallel convergence or divergence and the overall low diversity of fault types suggest a more planar fault surface. The dominance of transport-parallel strike slip within the Norwegian thrust sheet suggests substantial along-strike variation in the amount of transport that is accommodated by minor faults. Although there are many similarities in the character of the mesoscale deformation observed within each of the thrust sheets, these differences illustrate the complexity of the mesoscale-faulting style of deformation.

CONCLUSION

From our balanced cross section, we have determined a minimum of 60% (15 km) shortening of the Paleozoic section across the central Sawtooth Range. The shortening has been accommodated by a forward-developing imbricate fan with primary décollement horizons that are present at the base of the Devonian Jefferson Formation, in the Mississippian Allan Mountain Formation, and in the Cretaceous Colorado Group.

Mesosopic deformation within the Paleozoic carbonate rocks exposed within the central Sawtooth Range was accommodated by the progressive development of mesoscopic fault arrays which allowed the base of the thrust sheet to deform by cataclastic flow. Regional fault zones widen progressively, with the thickness of the BDZ increasing linearly as a function of increased thrust displacement. This indicates that BDZ development and thrust-sheet emplacement are temporally and genetically related. This empirical correlation may be limited to thrust sheets that contain similar rock types and that deformed under similar environmental conditions by similar processes. BDZ thickness is independent of fault shape, but the kinematics of the faults within the zone are not. BDZ thickness is not a function of subsequent foreland deformation, suggesting that little reactivation of these fault surfaces occurs during piggyback motion.

Even though the intensity of mesoscale de-

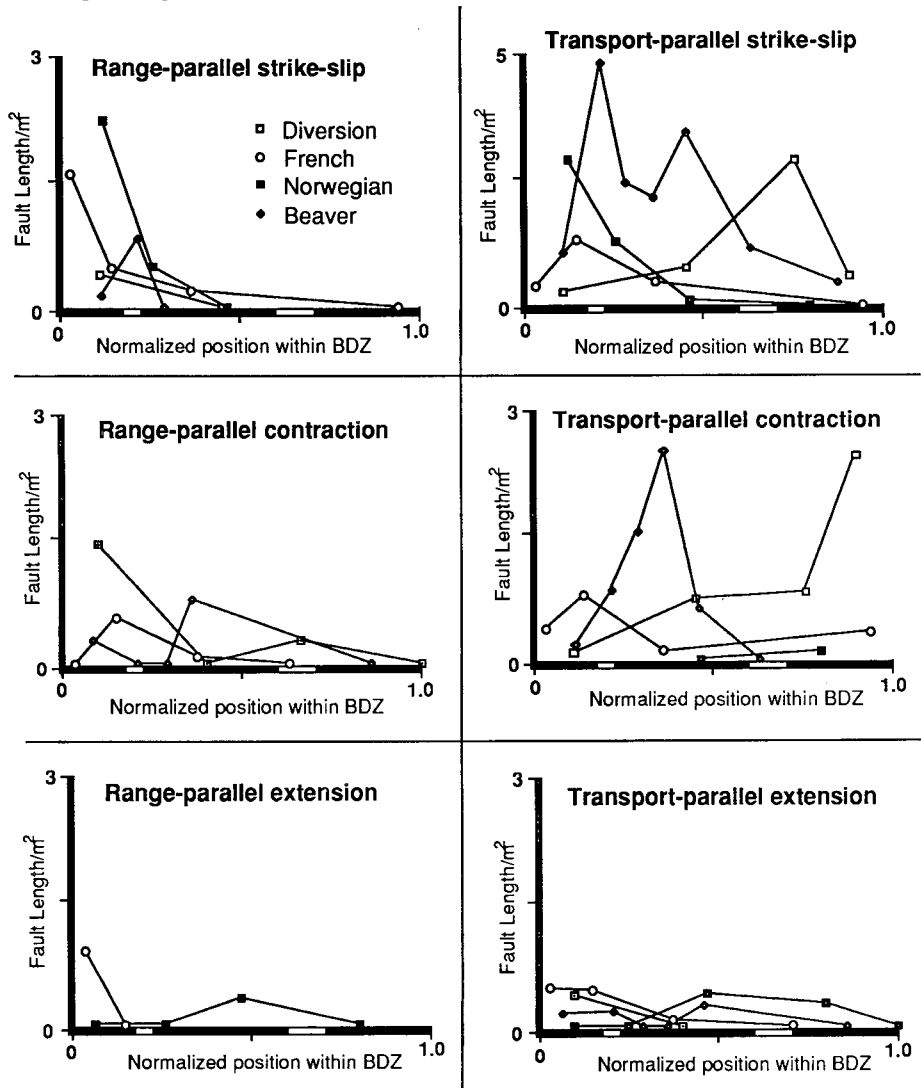


Figure 15. Graph showing the variations in the intensity of the individual fault populations as a function of normalized position within all BDZs studied. Breaks in the x-axis indicate boundaries between the three regions of the BDZs.

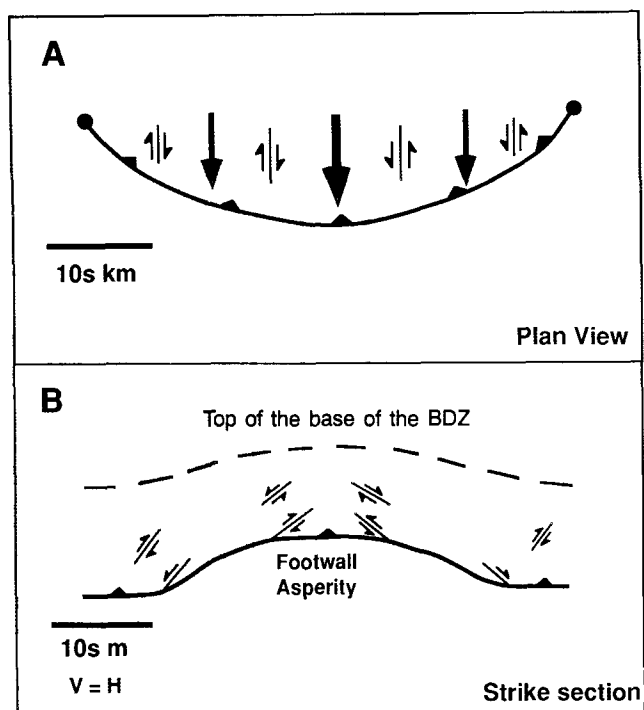


Figure 16. (A) Map view of the types of tear faults expected in a thrust sheet that has its maximum displacement at its center, with displacement decreasing towards the lateral terminations. (B) Sketch of possible minor faults that may develop in response to movement of the hanging wall over asperities in footwall.

formation is always higher at the base than at the top of the BDZ, the pattern of decreasing fault intensity is not always a simple one. Zones of intense faulting may occur within the BDZ, producing peaks in the overall pattern. At the base of a BDZ, a high diversity of minor fault types accommodates strike-parallel contraction and extension, variations in thrust-sheet displacement, and simple shear within the thrust sheet. At the top of the BDZs, a lower diversity of minor faults are dominantly dip- or strike-slip and accommodate simple shear or along-strike variations in thrust-sheet displacement. Only at the top of the BDZs do minor faults mimic the regional kinematics. The results of this analysis provide a caution to workers attempting to interpret regional kinematics from minor faults.

ACKNOWLEDGMENTS

This research was carried out as part of James Holl's M.S. thesis at Lehigh University. Field work was supported by grants from the American Association of Petroleum Geologists, Sigma Xi, and Standard Oil of California. The authors

would like to thank Geosource Inc. for supplying the seismic data, the Montana Bureau of Mines for supplying well logs, and the U.S. Forest Service for logistic support. Reviews by A. Sylvester, S. Boyer, S. Wojtal, and D. Spratt greatly improved this manuscript.

REFERENCES CITED

- Aleksandrowski, P., 1985, Graphical determination of principal stress direction populations: An attempt to modify Arthaud's method: *Journal of Structural Geology*, v. 7, p. 73-82.
- Anastasio, D. J., 1987, Thrusting, halotectonics and sedimentation in the External Sierra, Southern Pyrenees, Spain [Ph.D. dissert.]: Baltimore, Maryland, Johns Hopkins University.
- Anderson, E. M., 1951, The dynamics of faulting and dyke formation with applications to Britain: London, England, Oliver and Boyd, 206 p.
- Angelier, J., 1979, Determination of the mean principal direction of stresses for a given fault population: *Tectonophysics*, v. 56, p. T17-T26.
- , 1984, Tectonic analysis of fault slip data sets: *Journal of Geophysical Research*, v. 89, p. 5835-5848.
- , 1989, From orientation to magnitudes in paleostress determinations using fault slip data: *Journal of Structural Geology*, v. 11, p. 37-50.
- Arthaud, F., 1969, Methode de determination graphique des directions de raccourcissement, d'allongement et intermediaire d'une population de failles: *Bulletin of the Geological Society of France*, v. 11, p. 729-732.
- Bally, A. W., Gordy, P. L., and Stewart, G. A., 1966, Structure seismic data, and orogenic evolution of southern Canadian Rocky Mountains: *Bulletin of Canadian Petroleum Geology*, v. 14, p. 337-381.
- Bielenstein, H. U., 1969, The Rundle thrust sheet, Banff, Alberta [Ph.D. dissert.]: Kingston, Ontario, Queen's University.
- Elliott, D., 1976, The energy balance and deformation mechanisms of thrust sheets: *Philosophical Transactions of the Royal Society of London*, ser. A, v. 283, p. 289-312.
- , 1983, The construction of balanced cross section: *Journal of Structural Geology*, v. 5, no. 2, p. 101.
- Eichcopf, A., Vasseur, G., and Daignieres, M., 1981, An inverse problem in microtectonics for the determination of stress tensors from fault striation analysis: *Journal of Structural Geology*, v. 3, p. 51-65.
- Evans, J. P., 1990, Thickness-displacement relationships for fault zones: *Journal of Structural Geology*, v. 12, p. 1061-1065.
- Hoepfner, R., 1953, Faltung und Klüftung in nordteil des rheinischen schiefergebirges: *Geologische Rundschau*, v. 41, p. 144.
- Holl, J. E., 1991, Deformation mechanisms and finite strain within the foreland imbricate fan, Sawtooth Range, Montana [M.S. thesis]: Bethlehem, Pennsylvania, Lehigh University, 55 p.
- Hull, J., 1988, Thickness-displacement relationships for deformation zones: *Journal of Structural Geology*, v. 10, p. 431-435.
- Mitra, S., 1986, Duplex structures and imbricate thrust systems: Geometry, structural position and hydrocarbon potential: *American Association of Petroleum Geologists*, v. 70, p. 1087-1112.
- Mudge, M. R., 1965, Bedrock geologic map of the Sawtooth Ridge quadrangle, Teton and Lewis and Clark counties, Montana: U.S. Geological Survey Geologic Quadrangle Map GQ-381, scale 1:62,500.
- , 1966, Geologic map of the Patricks Basin quadrangle, Teton and Lewis and Clark counties, Montana: U.S. Geological Survey Geologic Quadrangle Map GQ-453, scale 1:62,500.
- , 1970, Origin of the Disturbed Belt in northwestern Montana: *Geological Society of America Bulletin*, v. 81, p. 377-392.
- , 1972, Structural geology of the Sun River Canyon and adjacent areas northwestern Montana: U.S. Geological Survey Professional Paper 663-B, 52 p.
- , 1982, A resume of the structural geology of the northern disturbed belt, Northwestern Montana, in Blake, R., ed., *Rocky Mountain Association of Petroleum Geologists—Geologic Studies of the Cordilleran Thrust Belt*, v. 1, p. 91-122.
- Mudge, M. R., and Earhart, R. L., 1983, Bedrock geologic map of part of the Northern Disturbed Belt, Lewis and Clark, Teton, Pondera, Glacier, Flathead, Cascade, and Powell Counties, Montana: U.S. Geological Survey Miscellaneous Investigation Series Map I-1375, scale 1:125,000.
- Mudge, M. R., Earhart, R. L., Whipple, J. W., and Harrison, J. E., 1982, Geologic and structure map of the Choteau 1° x 2° quadrangle western Montana: U.S. Geological Survey Miscellaneous Investigation Series Map I-1300, scale 1:125,000.
- Norris, D. K., 1958, Structural conditions in Canadian coal mines: *Geological Survey of Canada Bulletin*, v. 44, p. 1-54.
- Otsuki, K., 1978, On the relationship between the width of shear zone and the displacement along a fault: *Journal of the Geological Society of Japan*, v. 84, p. 661-669.
- Platt, J. P., and Leggett, J. K., 1986, Stratal extension in thrust footwalls, Makran accretionary prism: Implications for thrust tectonics: *American Association of Petroleum Geologists*, v. 70, p. 191-203.
- Price, R. A., 1967, The tectonic significance of mesoscopic subfabrics in the southern Rocky Mountains of Alberta and British Columbia: *Canadian Journal of Earth Sciences*, v. 4, p. 39-70.
- Reches, Z., 1978, Analysis of faulting in a three-dimensional strain field: *Tectonophysics*, v. 47, p. 109-129.
- , 1987, Determination of the tectonic stress tensor from slip along faults that obey the Coulomb yield condition: *Tectonics*, v. 6, p. 849-861.
- Robertson, E. G., 1983, Relationship of fault displacement to gouge and breccia thickness: *Mining Engineering*, v. 35, p. 1426-1432.
- Serra, S., 1977, Styles of deformation in the ramp regions of overthrust faults: *Annual Field Conference*, 29th, Jackson, Wyoming, Wyoming Geological Association Guidebook.
- Stearns, D. W., 1969, Fracture as a mechanism of flow in naturally deformed layered rocks: *Geological Survey of Canada Special Paper* 68-52, p. 79-95.
- Twiss, R. J., and Geffell, M. J., 1990, Curved slickenfibers: A new brittle shear indicator with application to a sheared serpentinite: *Journal of Structural Geology*, v. 12, no. 4, p. 471-481.
- Wallace, R. E., 1951, Geometry of shearing stress and relation to faulting: *Journal of Geology*, v. 59, p. 118-130.
- Wojtal, S., 1986, Deformation within foreland thrust sheets by populations of minor faults: *Journal of Structural Geology*, v. 8, p. 341-360.
- , 1989, Measuring displacement gradients and strain in faulted rocks: *Journal of Structural Geology*, v. 11, p. 669-678.
- Wojtal, S., and Mitra, G., 1986, Strain hardening and strain softening in fault zones from foreland thrusts: *Geological Society of America Bulletin*, v. 97, p. 674-687.
- Wojtal, S., and Pershing, J., 1991, Paleostresses associated with faults of large offset: *Journal of Structural Geology*, v. 13, p. 49-62.
- Woodward, N. B., Wojtal, S., Paul, J. B., and Zadins, Z. Z., 1988, Partitioning of deformation within several external thrust zones of the Appalachian Orogen: *Journal of Geology*, v. 96, p. 351-361.

MANUSCRIPT RECEIVED BY THE SOCIETY MARCH 25, 1991
 REVISED MANUSCRIPT RECEIVED DECEMBER 2, 1991
 MANUSCRIPT ACCEPTED DECEMBER 6, 1991